Supplementary Information (SI) for Journal of Materials Chemistry A.
This journal is © The Royal Society of Chemistry 2024

Supporting Information

High-energy density dielectric film capacitors enabled by grain boundary engineering

Yupeng Liu ,[a] Tian-Yi Hu ,[a] Ming Liu,[b] Rui Lu ,[ab] Lu Lu ,[c] Yiqin Lu,[b] Qiuyang Han ,[b] Weijie Fu ,[a] Tingzhi Duan ,[b] Yanzhu Dai ,[b] Chunrui Ma ,*[a] Shao-Bo Mi *[cd] and Chun-Lin Jia [b]

[a] *State Key Laboratory for Mechanical Behavior of Materials and School of Materials Science and Engineering, Xi'an Jiaotong University, Xi'an, 710049, China*

[b] *School of Microelectronics, Xi'an Jiaotong University, Xi'an, 710049, China*

[c] *Ji Hua Laboratory, Foshan, 528200, China*

[d] *Foshan University, Foshan, 528225, China*

***Corresponding authors:**

E-mail: chunrui.ma@xjtu.edu.cn (C.R. Ma), mishaobo@jihualab.ac.cn (S.-B. Mi)

Supplementary Text

1. Weibull Distribution:

According to the fitting formula $P(E)=1-\exp\left[-\left(\frac{E}{E_b}\right)^{\beta}\right]$, the following formula can be derived.

$$\lg\left[Ln\left(\frac{1}{1-P_i}\right)\right]=\beta\left[\lg\left(E_i-\lg\left(E_b\right)\right)\right] \tag{S1}$$

* MERGEFORMAT (S1)

$$X_i=\lg\left(E_i\right) \tag{S2}$$

* MERGEFORMAT (S2)

$$Y_i=\lg\left[Ln\left(\frac{1}{1-P_i}\right)\right] \tag{S3}$$

* MERGEFORMAT (S3)

$$P_i=\frac{i}{n+i} \tag{S4}$$

* MERGEFORMAT (S4)

Where n represents the total tested points, E_i represents the breakdown field strength when the ith points is tested in ascending order $\left(E_1\le E_2\le E_3 \ldots \le E_n\right)$, E_b is the characteristic breakdown strength, β is the value of the slope of the linear fit of the data Y_i and X_i, P_i is the cumulative probability of electric failure. Generally, the larger value indicates that the range of fluctuation of the breakdown data is smaller, and the calculated breakdown field strength E_b is more reliable. In this work, we select 15 breakdown points for linear fitting to obtain breakdown strengths.[1, 2]

2. Analyzing the leakage mechanisms in the BT-BMZ films

The conduction mechanism of the BT-BMZ films can be characterized by the leakage current fitting results with the following formulas:

Ohmic conduction:

$$J = \sigma E$$ * MERGEFORMAT (S5)

Space-charge-limited conduction (SCLC):

$$J = \frac{9\mu\varepsilon_0\varepsilon_r}{8} \cdot E^2$$ * MERGEFORMAT (S6)

P-F emission:

$$J = e\mu N_c E \cdot \exp\left[-\frac{\Phi_{PF}}{k_B T} + \frac{1}{k_B T}\left(\frac{e^3 E}{\pi\varepsilon_0 K}\right)^{1/2}\right]$$ * MERGEFORMAT

(S7)

Schottky emission:

$$J = AT^2 \cdot \exp\left[-\frac{\Phi_{schottky}}{k_B T} + \frac{1}{k_B T}\left(\frac{e^3 E}{4\pi\varepsilon_0 K}\right)^{1/2}\right]$$ * MERGEFORMAT

(S8)

Where J , E, σ, μ, e, ε_0, ε_r, A, Φ_{PF}, T, k_B, $\Phi_{Schottky}$, K, and N_c represent the leakage current density, the applied electric field, electric conductivity, electronic drift mobility, electronic charge, vacuum permittivity, relative permittivity, Richardson constant, P-F emission energy barrier, absolute temperature, Boltzmann constant , Schottky energy barrier, optical permittivity, and effective density of states of the conduction band, respectively. Note that the optical permittivity K equals to n^2 (n is the refractive index).[1, 3, 4]

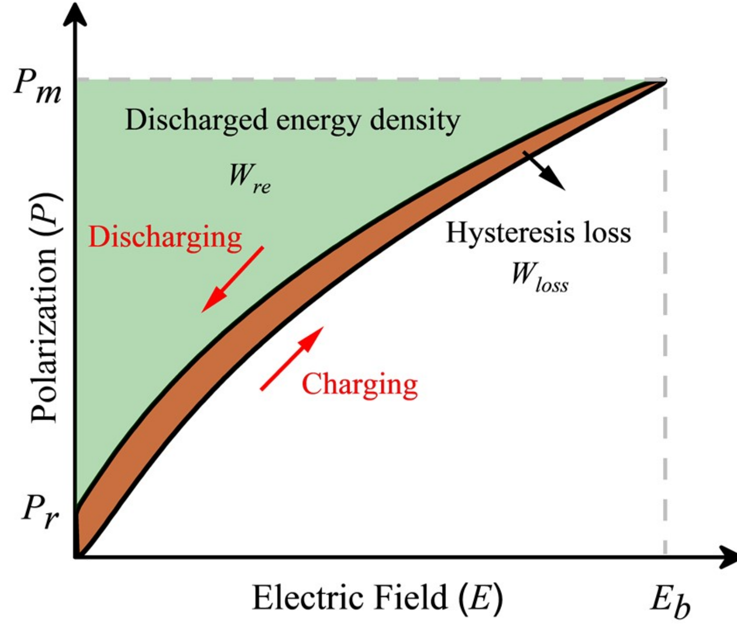

Fig. S1 Schematic of dielectric energy storage. Dielectric energy storage capacitors are designed to store energy by charging and discharging through the process of polarization and depolarization of the dielectric in an applied electric field.

$$W_{re} = \int_{P_r}^{P_m} E dP \qquad \text{* MERGEFORMAT (S9)}$$

The discharge energy density W_{re} is represented by the green region, where P_m and P_r are the maximum and residual polarization, respectively. The energy storage efficiency η can be calculated from the following equation:

$$\eta = \frac{W_{re}}{W_{re} + W_{loss}} \qquad \text{* MERGEFORMAT (S10)}$$

The yellow region represents the energy loss W_{loss} due to hysteretic polarization switching in the charge-discharge cycle, and E_b denotes the breakdown strength, i.e., the highest electric field that the dielectric can withstand.[5]

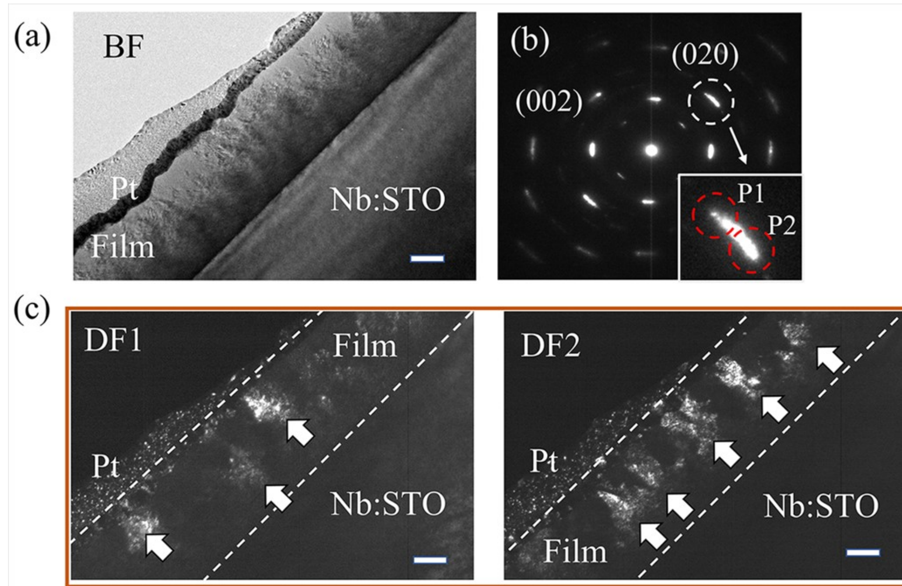

Fig. S2 (a) Bright-field TEM image and (b) the corresponding SAED pattern of the BT-BMZ film prepared under 0.170 mbar growth pressure, recorded along the $[100]$ zone axis. (c) The dark-field TEM image (DF1 & DF2) obtained by using P1 and P2 diffraction arcs indicated by red circles in (b), respectively. The nanocolumnar grains are marked by the white arrows in the film. The scale bar is 100 nm.

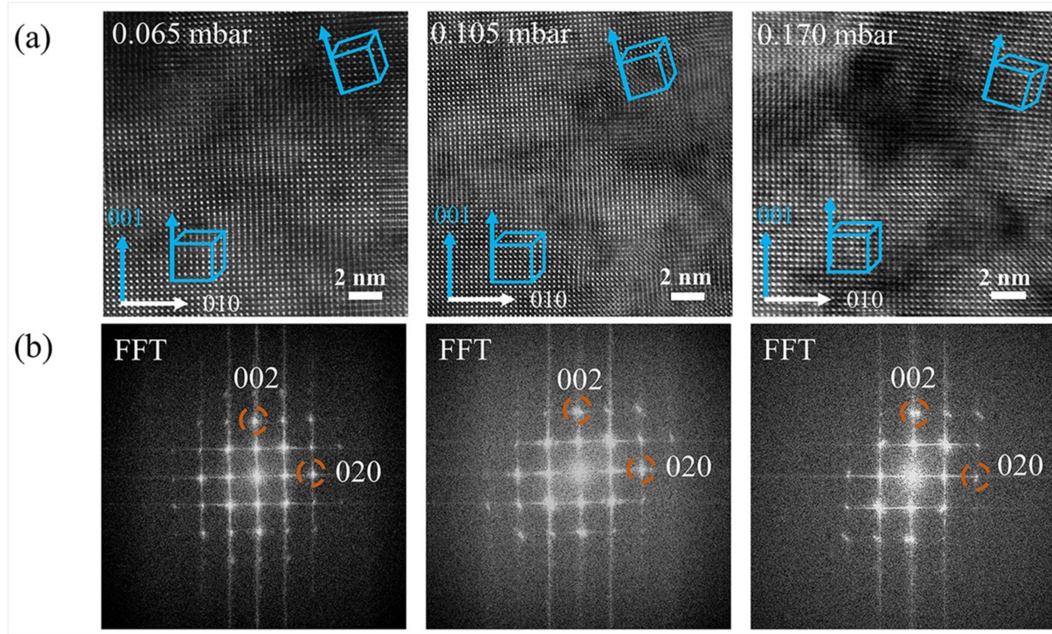

Fig. S3 (a) High-resolution HAADF-STEM images of the BT-BMZ films prepared under 0.065 mbar, 0.105 mbar, and 0.170 mbar, recorded along the $[100]_{film}$ zone axis, respectively. (b) The corresponding Fast Fourier Transform (FFT) patterns of (a). Note that the tilting between adjacent grains can be visible in (a), as illustrated by the inserts superposed on the images. As a result, the splitting of spots occurs in the FFT patterns in (b), as marked by open circles.

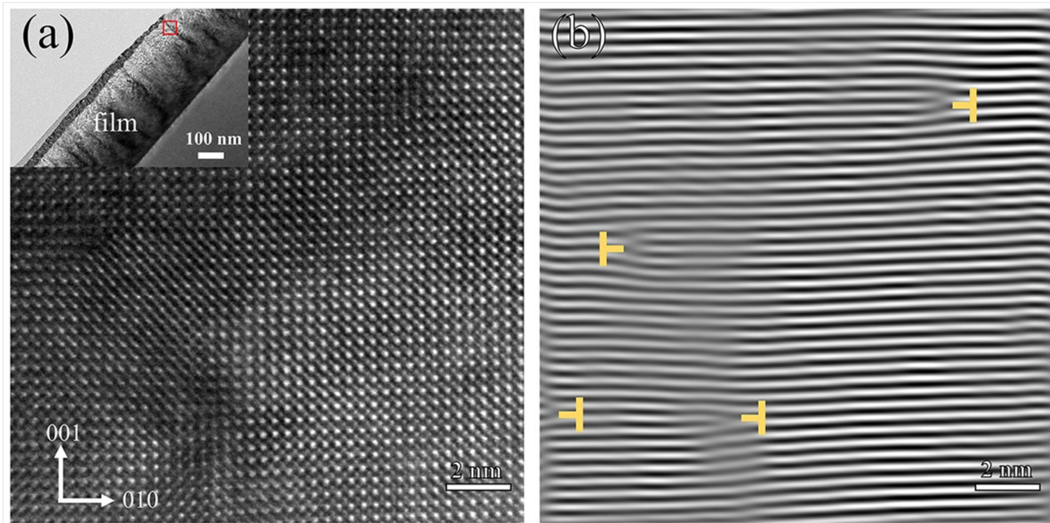

Fig. S4 (a) Atomic-resolution HAADF-STEM image of the grain boundary in the BT-BMZ film prepared under 0.065 mbar growth pressure. The insert is the low-magnification morphology of the BT-BMZ film. (b) The Inverse Fast Fourier Transform image of (a) showing the formation of dislocations along the grain boundary.

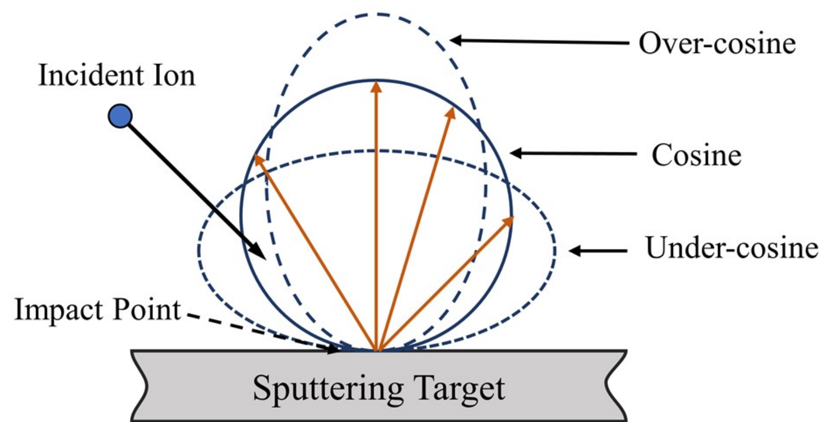

Fig. S5 Schematic diagram of the emission angle distribution of sputtered atoms.[6]

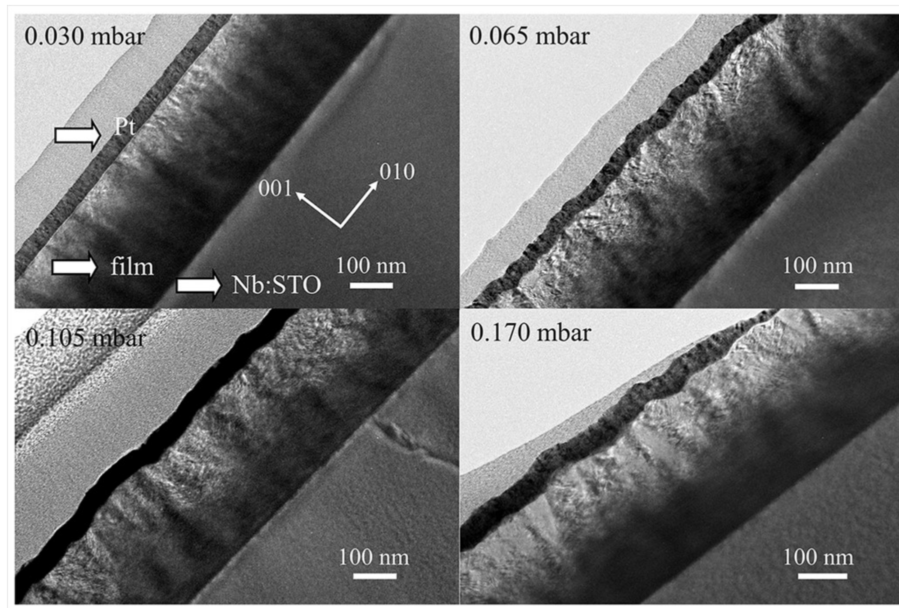

Fig. S6 Low-magnification cross-sectional TEM images of BT-BMZ film prepared under different growth pressures.

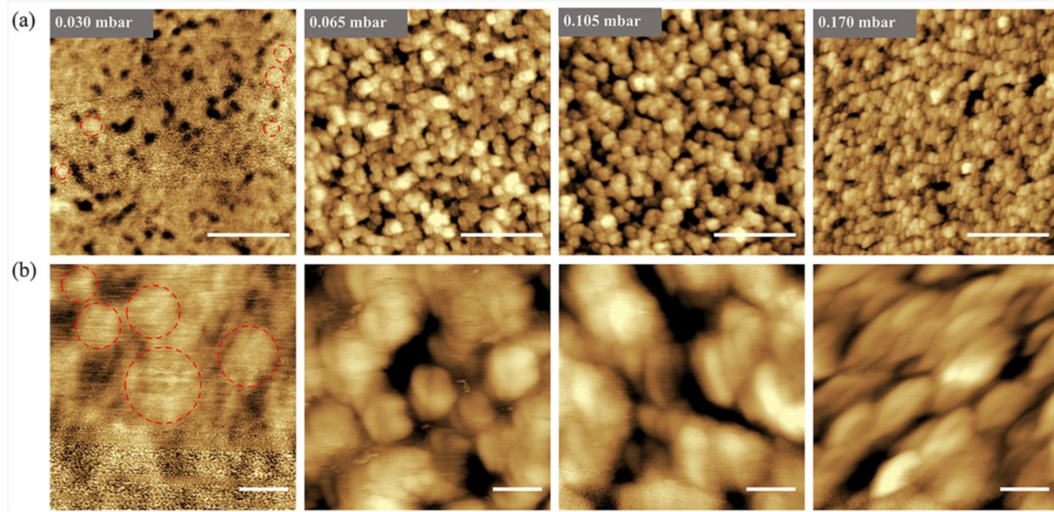

Fig. S7 (a) The AFM images ($3\mu m \times 3\mu m$) and (b) the enlarged view of AFM images ($0.5\mu m \times 0.5\mu m$) of BT-BMZ films prepared under different growth pressures. The scale bar in is 1 μm in (a) and 100 nm in (b), respectively.

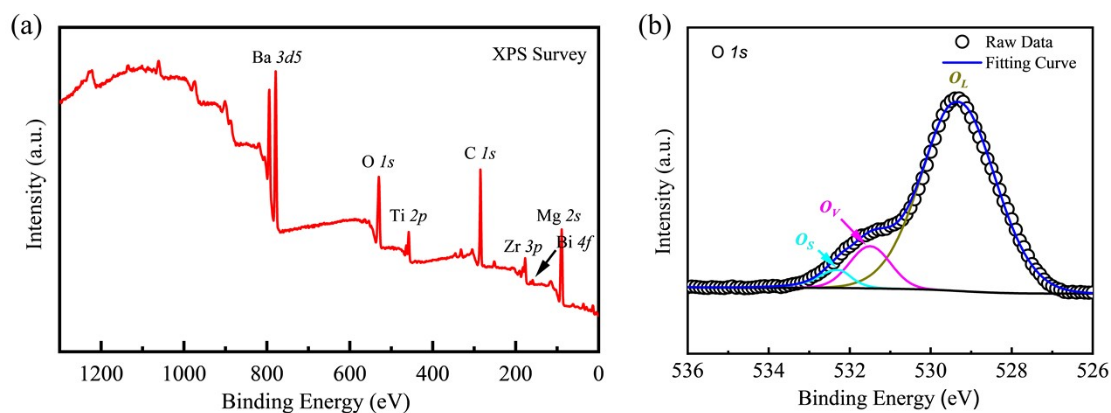

Fig. S8 (a) XPS survey spectrum and (b) O 1s XPS spectrum for the film prepared under 0.030 mbar growth pressure. As displayed in (a), the elemental compositions detected by XPS remain consistent with the BT-BMZ film. As shown in (b), the O 1s XPS spectrum of the film consists of three absorption peaks, where the 529.3 eV peak corresponds to the vibrational absorption peak of lattice oxygen (O_L), the 531.5 eV peak is attributed to the presence of oxygen vacancies (O_V) in the film, and the 532.3 eV peak represents absorbed oxygen or hydroxyl oxygen (O_S) on the film surface.[7, 8] The results of XPS experiments indicate the presence of oxygen vacancies in the BT-BMZ films.

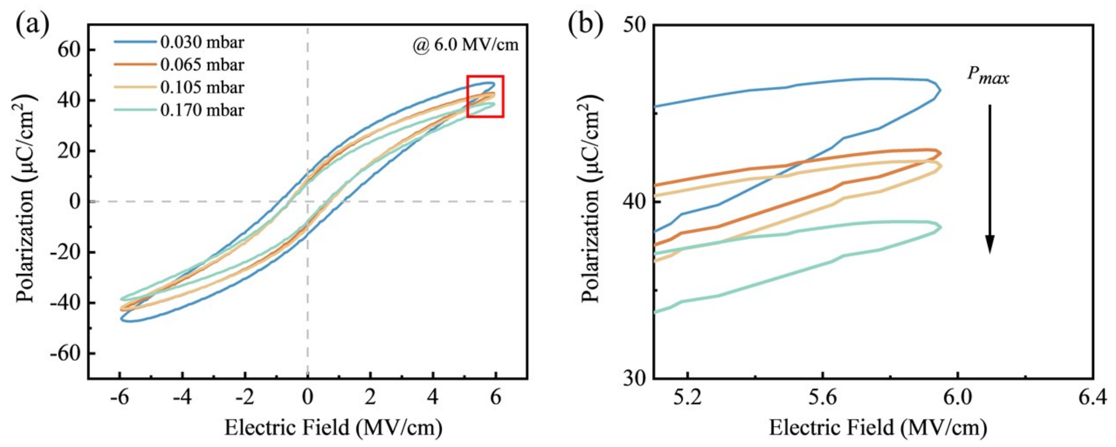

Fig. S9 (a) Bipolar *P*-*E* loops of BT-BMZ films under different growth pressures at the same electric field. (b) An enlarged view of region of interest (ROI) in (a) showing the change of P_{max} under different film growth conditions.

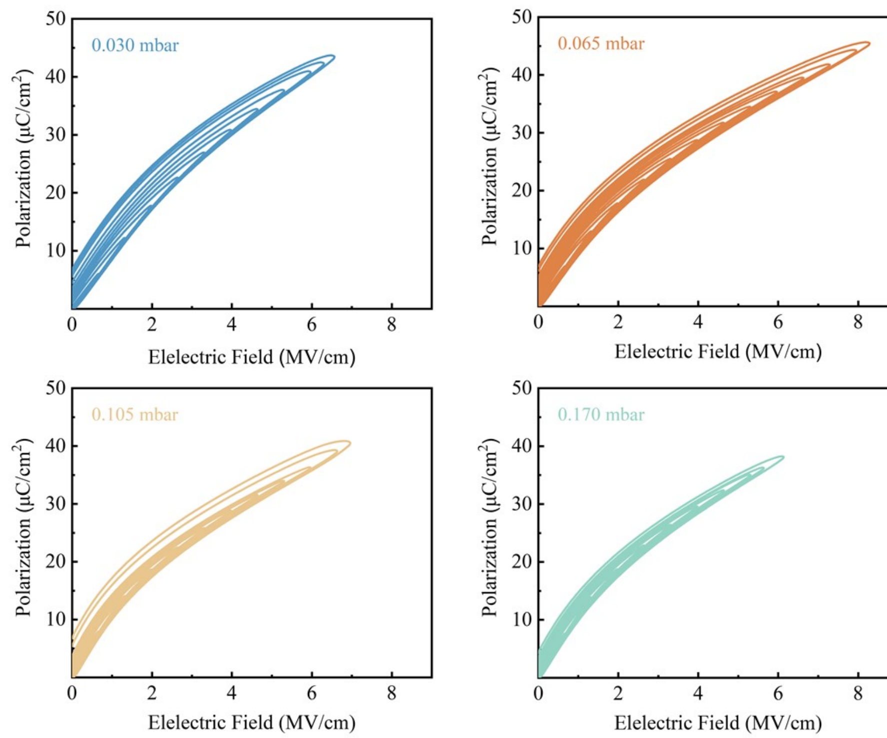

Fig. S10 Unipolar *P-E* loops of the BT-BMZ films at 1 kHz prepared under various growth pressures.

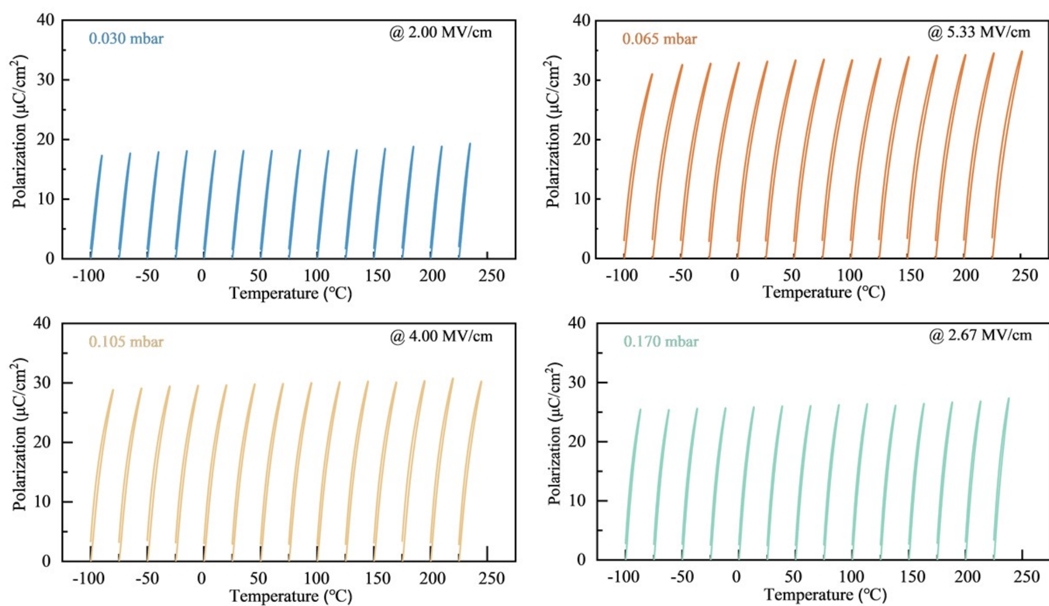

Fig. S11 Unipolar *P*-*E* loops of the BT-BMZ films measured at different temperatures.

References

1 H. Pan, S. Lan, S. Q. Xu, Q. H. Zhang, H. B. Yao, Y. Q. Liu, F. Q. Meng, E. J. Guo, L. Gu, D. Yi, X. R. S. Wang, H. B. Huang, J. L. MacManus-Driscoll, L. Q. Chen, K. J. Jin, C. W. Nan and Y. H. Lin, *Science*, 2021, **374**, 100-104.

2 H. Pan, J. Ma, J. Ma, Q. Zhang, X. Liu, B. Guan, L. Gu, X. Zhang, Y. J. Zhang, L. Li, Y. Shen, Y. H. Lin and C. W. Nan, *Nat. Commun.*, 2018, **9**, 1813.

3 H. Pan, F. Li, Y. Liu, Q. H. Zhang, M. Wang, S. Lan, Y. P. Zheng, J. Ma, L. Gu, Y. Shen, P. Yu, S. J. Zhang, L. Q. Chen, Y. H. Lin and C. W. Nan, *Science*, 2019, **365**, 578-582.

4 F.-C. Chiu, *Adv. Mater. Sci. Eng.*, 2014, **2014**, 1-18.

5 H. Palneedi, M. Peddigari, G.-T. Hwang, D.-Y. Jeong and J. Ryu, *Adv. Funct. Mater.*, 2018, **28**, 1803665.

6 in *Thin Films*, eds. R. A. Powell and S. M. Rossnagel, Elsevier, Amsterdam, The Netherlands, 1999, vol. 26, ch. 2, pp. 23-49.

7 J. L. Lin, R. He, Z. Lu, Y. Lu, Z. Wang, Z. Zhong, X. Zhao, R.-W. Li, Z. D. Zhang and Z. J. Wang, *Acta Mater.*, 2020, **199**, 9-18.

8 Y. Liu, H. Han, H. Pan, S. Lan, Y. Lin and J. Ma, *J. Alloys Compd.*, 2023, **937**, 168452.